Quarterly Report to the
PHMSA, US Dept. of Transportation
Interagency Agreement DTRS56-04-X-0025
April 30, 2004 as Modified August 4, 2004

Task Order #02
Fatigue Fracture and Crack Arrest in High-Strength Pipeline Steels
For the Quarter ending
March 31, 2006

1. **Progress, Findings, and Activities:**
   a) Task 1 Standards – Active on ASTM Committees E08 and E28 (mechanical Testing) to keep abreast of ASTM Standards appropriate for use by the pipeline industry.

   b) Task 2 Fatigue and Fracture – As a precursor to the fatigue work, standard tensile testing was conducted on the pipe sections supplied to us by two pipeline operators. In addition to the low to mid-strength materials received from PG&E that were previously reported, this report contains data on the X65 and X100 high strength steel pipelines supplied by British Petroleum (BP). Data from this task is supplied in the attached appendix.
   One of the main objectives of this quarter was to complete the fatigue testing on the pipeline specimen materials obtained from PG&E and British Petroleum. We received the pipeline sections from PG&E and BP and machined them into appropriately sized full-thickness (where possible) fatigue specimens. The PG&E pipes are 20 to 25 in. in diameter and have wall thicknesses of 5/16" and 3/8". The BP pipeline sections were 20-52 inches in diameter and range in thickness from 1.0" to 1.5". The fatigue specimens are oriented along the axis of the pipe length and the fatigue crack is transverse to the axial direction (hoop direction) of the pipe. The fatigue specimens are hourglass shaped and have a test section width of 4" and a reduced section length of 6". A ½" wide notch was electrical discharge machined in the center of the specimens as a starter for the fatigue pre-crack. The specimens were fatigue pre-cracked to a predetermined length and then fatigued while recording fatigue crack growth rate data. Examples of the FCGR data can also be seen in the attached appendix.

   Another focus during this period was to conduct Crack-Tip Opening Angle Testing (CTOA) on the supplied pipeline materials. CTOA, originally based on the COD ductile fracture criterion, has been proposed as a fracture parameter in line-pipe steels as a measure of dynamic, ductile, and steady-state fracture toughness. CTOA specimens were machined from the pipeline sections with the notch and fatigued pre-crack aligned with the axial direction of the pipes. The specimens were typically machined to be 3 mm thick because of the wall thickness and curvature of the pipe wall and a desire not to flatten the sections for testing. Some of the thicker, larger diameter pipelines permitted the machining of 8mm thick specimens, allowing us to evaluate the effects of

specimen thickness on CTOA. The specimens were 100mm wide and 200 mm long. A notch, 60 mm long from the load centerline, was machined in the front edge of the specimens to facilitate a 2-4 mm pre-crack. In addition, we machined one API-5L-X100 steel CTOA specimen with the notch oriented so that the crack would grow across the transition from base metal to heat-affected zone to weld metal and then back into the HAZ and base metal. This specimen gave us an idea as to the ductile fracture characteristics of the weld metal/HAZ area. Sample test results from the fatigue and CTOA experiments are included in the appendix this report.

We hosted two pipeline research related meetings in Boulder in January, 2006; the first was held January 23 and 24 to discuss our work related to high strength pipeline steels. This closed meeting was co-hosted by BP and was attended by participants from across the US as well as Canada, Italy and the UK. Results from this meeting heightened our awareness of the importance of strain-based design in new high strength pipeline steels. BP has offered more steels (welds and base metals) in support of our research efforts. Other collaborations are being developed as a result of this meeting (Yong-Yi Wang and Gery Wilkowski (EMCC), Gianluca Manucci (Italy), and Brian Leis (Batelle)). The second meeting, the PHMSA/NIST Welding and Joining Workshop was held January 25 and 26. This workshop had 69 participants representing pipeline ownwers, technology developers, trade and standards organizations, and government agencies. The workshop structure included six keynote presentations to suggest some issues, five working groups (by topical area) to identify and rank the research needs, and summary presentations (back to the whole group) to compare results and comment on any overlaps or omissions. The output includes a list of 18 priority goals for additional research in topical areas of Weld Design, Construction, Weld Inspection and Assessment, Weld Maintenance and Repair, and Joining Issues for Nonmetallic Materials. The proceedings are already on the PHMSA website, and are being collected on a CD for broad distribution.

British Petroleum provided us with a previously tested full-sized pipe section of API-5L-X100. The pipe section is about 25 feet long, 52” diameter and has a wall thickness of slightly less than 1 inch. In addition to this section, they also sent us some fractured pieces from the tested pipe, and another section that was about 4 feet long with a diameter and wall thickness to match the above described pipe. We torch cut a number of pieces from this short section in order to make tensile, fatigue and CTOA specimens. We also sent a piece, approximately 2’X2’, to Chris San Marchi of Sandia Livermore Labs, for his experiments on high pressure hydrogen testing. We also received some API-5L-X65 pipeline steels from BP in three different wall thicknesses and diameters.

We had two attendees at the October meeting of the PRCI held in Galveston, TX. While there, we had a number of helpful technical discussions and

interactions with other attendees, affirming our research direction. We also discussed our proposed plan to conduct high rate CTOA tests on full-thickness pipeline specimens using equipment available at NIST-Boulder. This information, combined with the Kolsky testing in Gaithersburg, would be valuable for the strain based design of pipelines currently being funded by the PRCI and DOT.
We also attended the PHMSA Mechanical Damage Technical Workshop held in Houston in February 2006, and as recommended by the findings of this workshop, continue to reach out for collaboration in our research efforts.

1. Activities Planned for the Next Reporting Period:

a). Task 1 Standards: Continue to interact with ASTM committees E08 and E28.

b). Task 2 Fatigue: We will continue our FCGR program, generating fatigue data for a database on pipeline steels. Included in this database will be further FCGR data (axial fatigue crack orientation) on the API-5L-X100 and the API-5L-X65 pipeline steels provided by BP. In addition we plan to conduct fatigue testing along and/or across welds on the X100 steel, as well as conduct fatigue testing on pipeline specimens damaged using a controlled, repeatable method for application of damage.

c). Task 3 Crack Arrest: Our work on ductile fracture crack resistance will continue through our efforts in CTOA testing. We have completed the CTOA work on the PG&E steels and plan to continue work on the X65 and X100 grades of steel and the girth weld associated with the X100 pipe material. We will be conducting CTOA tests on a variety of thicknesses to measure the effects of thickness on this measurement technique. After discussions with other pipeline researchers we found that there is a need for high rate CTOA testing on high-strength pipeline steels. While the drop weight tear test is adequate for testing the ductile fracture properties of lower strength steels, it is inadequate for the high-toughness, high-strength pipeline steels proposed for use today. We have planned future work on the effects of high strain rate on high strength pipeline steels using CTOA. This type of dynamic testing will most likely simulate the actual running crack conditions seen in a pipeline undergoing ductile fracture.

d). Task 4 Hydrogen Charged Fatigue: Working with researchers at Colorado School of Mines to understand the effect of fatigue rate on hydrogen property reduction.

e). Task 5 Support of OPS Programs: Continue to support pipeline safety efforts by participating in PSIA quarterly meetings and meetings with industry (e.g. IPC and PRCI)

f). Task 6: Fatigue Crack Growth at Third Party Damage: Now that we have characterized the basic fatigue behavior of various pipeline steels, we can apply controlled amounts of third-party damage to the specimens and measure the effect on the fatigue life.

g). Meetings and Committee Activities: NIST continues to support the pipeline R&D community through participation and organization of meetings, standards committee activities, and through participation in the interagency PSIA coordinating committee. We plan to continue our attendance at the PRCI meetings and DOT workshops, enabling us to keep abreast of the most current needs of the pipeline community. We have submitted two papers for presentation at the IPC2006 to be held in Calgary, Canada in September 2006.

h). Future Work:

Database: We will add a pipeline database to our web site to include publicly available data on pipeline properties. Initially this will be mostly the data generated from our fatigue and CTOA work in FY 04 and 05, and will include the Welding and Joining Workshop reports. We will continue to update it with the data generated in FY 06 and beyond.

Hydrogen charged fatigue crack growth - One higher strength and one lower strength pipeline section specimen, chosen from pipeline sections tested in Task 1, above, will be charged with hydrogen, coated, and fatigued in order to evaluate the effects of hydrogen on the fatigue crack growth properties of pipeline steels. (This has already been started in conjunction with Colorado School of Mines. The tests were designed in first quarter FY06, and specimens were received from the machine shop in second quarter FY06.) Data from these pre-charged high strength steel pipeline specimens will provide a fatigue database for hydrogen charged steels that will eventually be compared to available fatigue data taken under similar conditions (gaseous hydrogen pressures).

Strain-based design – We will develop measurement methods and techniques in support of strain-based design of high-strength pipeline steels. This will include analysis of tensile instability in support of other theories of pipeline fracture. Collaboration with other (outside) researchers is essential for this task to be successful.

Appendix

Mechanical properties

Uni-axial tensile properties

Table 1 list some tensile properties as obtained by the uniaxial test for the various pipes. In addition to the standard values, the ratios of $\sigma_{0.2}/\sigma_{UTS}$ and e_u/e_f are also given. These two parameters indicate the strain hardening potential of the steel. The highlighted numbers in the modulus column indicate the effect of the microcracking on the measured modulus derived from the stress-strain curve of the experimental test. The dynamic elastic modulus values (a more accurate method of modulus measurement) are shown in Table 2. As shown in figure 1, as the stress ratio increases, the strain ratio decreases, with a moderate trend for the T direction and a more steep trend for the L direction. The ratios of the various pipes are also given on the both L and T curves.

Table 1. Standard mechanical properties at L and T orientations for the tested pipes

Pipe	No	Orientation	E GPa	$\sigma_{0.2}$ MPa	σ_{UTS} MPa	$\sigma_{0.2}/\sigma_{UTS}$	e_u %	e_f %	e_u/e_f	Remarks
1	1	L	215	520	615	0.85	7.2	34.8	0.2	Unused pipe
	2	L	205	510	608	0.84	7.2	35.1	0.2	
	1	T	221	555	603	0.92	8.6	27	0.31	
	2	T	227	535	609	0.88	8.8	27.7	0.32	
2	1	L	**U180U**	375	556	0.67	12.4	31.2	0.35	X52
	2	L	**175**	360	557	0.65	12.8	34	0.37	
	1	T	207	460	573	0.80	10.2	25.6	0.40	
	2	T	216	445	578	0.77	10	25.5	0.39	
3	1	L	**U195U**	245	450	0.54	19.5	37.4	0.52	GRB
	2	L	**U195U**	245	451	0.54	19	38.2	0.5	
	1	T	202	260	460	0.56	20	38.7	0.52	
	2	T	197	255	458	0.56	19	37.3	0.51	
5	1	L	**1U80**	335	535	0.62	14	35.1	0.4	No I.D.
	2	L	**1U81**	335	536	0.62	13	34.7	0.38	
	1	T	207	425	559	0.76	9.6	21.9	0.44	
	2	T	205	427	561	0.76	9.4	22	0.43	
6	1	L	206	272	455	0.6	17.4	37.8	0.46	?
	2	L	205	288	459	0.63	17.5	38.2	0.46	
	1	T	208	250	455	0.55	19	33	0.58	
	2	T	196	250	453	0.55	19.2	37	0.52	

The following modulus measurements were made according to ASTM E 1876, using a dynamic elastic modulus measurement technique. These measurements were made on machined samples, with all microcracking removed from the samples.

Table 2. Dynamic modulus measurements on pipeline steels

Sample No.	Meas Date	E(1)	E(2)	E(4)	G(3)	μ
1	3/30/2005	212	210	211	82	0.284
2	3/30/2005	210	212	209	81	0.294
3	3/30/2005	213	211	211	82	0.287
4						
5	3/30/2005	210	211	209	82	0.284
6	3/30/2005	214	214	212	82	0.294
	Mean	212	212.6	211.1	82.5	0.289
	Std Dev	2.2	1.8	1.3	0.4	0.005

Mean E(all)	212	Adiabatic
Std Dev	1.24	
Est Isothermal		
E	207.5	Isothermal
±	1.24	

E(1)= Measured for out-of-plane flexure which has the greatest strains on the wide flat sides
E(2)= Measured for in-plane flexure which has the greatest strains on the long edges.
E(4)= Measured for longitudinal vibrations with equal strains across cross section.
G(3)= Shear modulus measured in torsion bending mode.

Note: All E measurements are in the long dimension of the sample.
Note: For 6.35 mm (1/4 in) thick steel the adiabatic to isothermal transition loading freq is about 1 Hz.

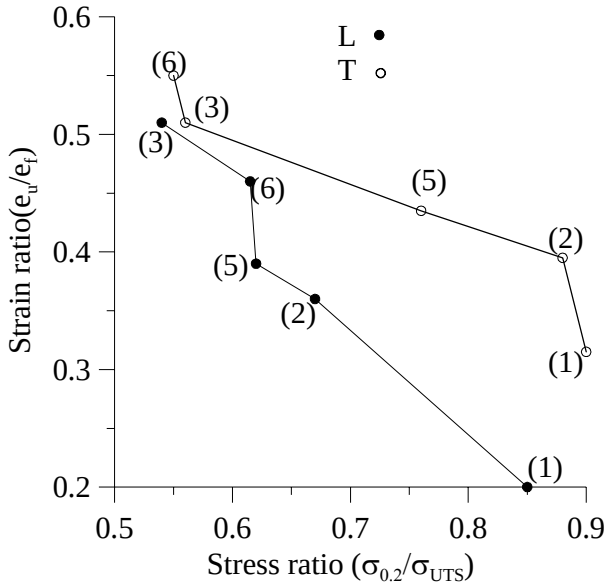

Figure 1. The dependency of the strain ratio with the stress ratio for both orientations.

Figures 2a and b summarize the values of the yield and the ultimate stresses in decreasing order for both directions and the appropriate uniform and total elongation respectively. As shown, pipe 1 exhibits the higher stresses with the lowest uniform elongation for the both directions. However, the lowest value for the total elongation was observed for pipe 5. Pipe 3 displays the lowest stresses with the highest uniform and total elongation. The most inconsistent trend for the total elongation in the T orientation for the uniform elongation was seen for pipe 2 and 5. This behavior is attributed to the preferred orientation, evident in the microstructure.

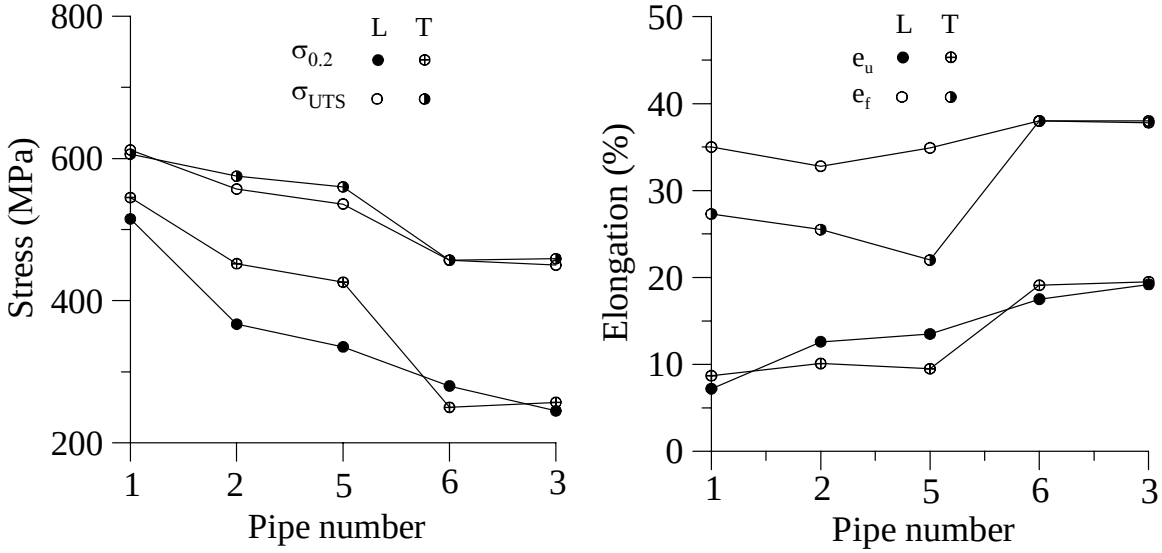

Figure 2. The highest through lowest yield and ultimate stress for both directions (a), and the respectively uniform and the total elongation (b).

The low Young's modulus (highlighted) obtained for pipes 2, 3 and 5 is attributed to the global damage of microcracking at the interior and exterior surfaces of the pipe due to the corrosion and stress corrosion cracking processes. Selected figures 3a,-d demonstrate such damage for the mentioned pipes. In pipe 3 (figures 8b-d) some crack–like features at the corrosion front and some areas that likely reflect corrosion within pearlite colonies were noticed more than in other pipes. In this pipe, it was not apparent that MnS stringers were preferred corrosion sites near the front.

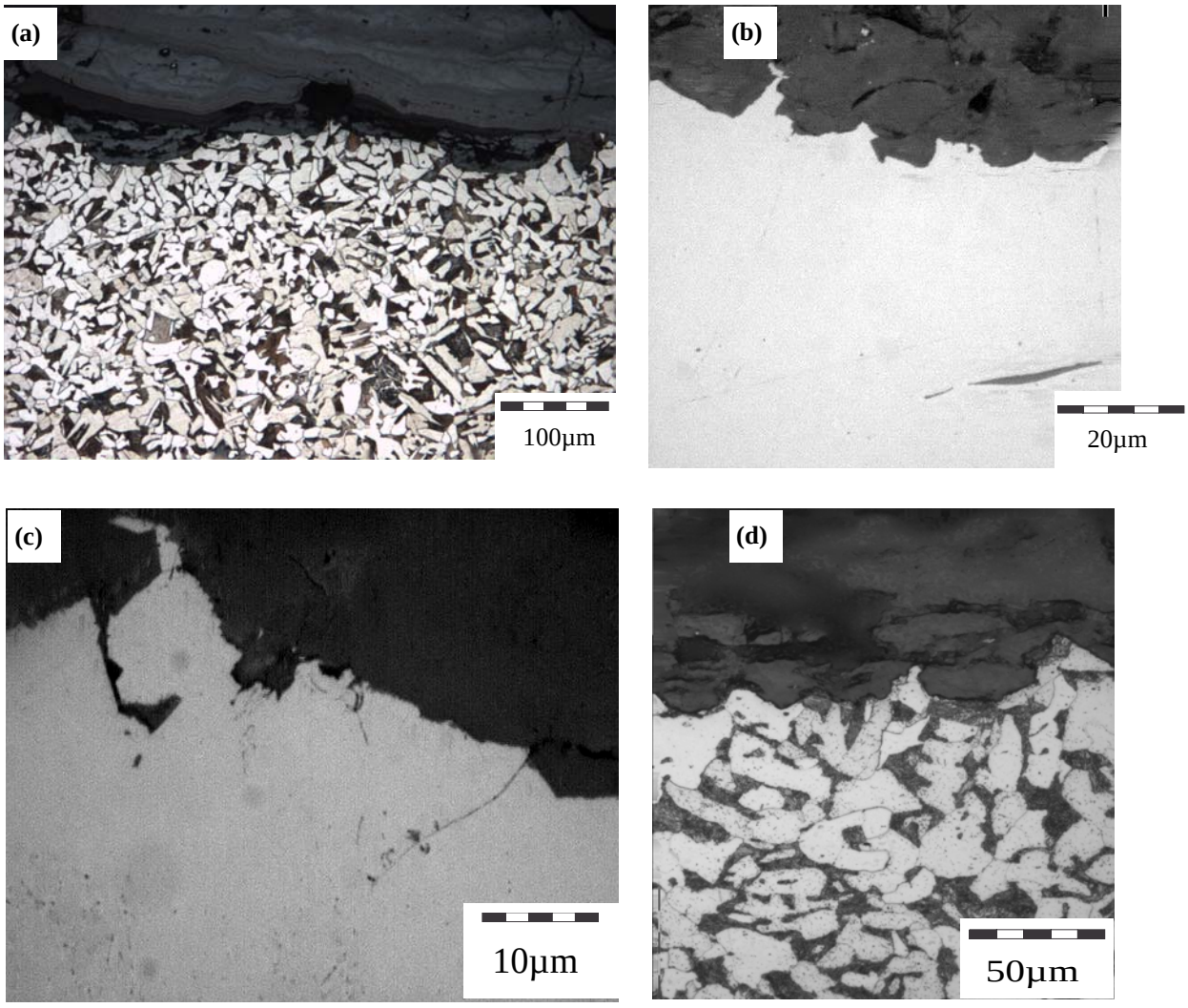

Figure 3. The corrosion and stress corrosion cracking in uniform general manners in selected pipes, (a) pipe 2, (c-b) pipe 3 , (d) pipe 5.

Although the original thickness is almost unaffected, the surface's which were damaged by the corrosion process exhibits microcracking while being stretched during the tensile test. In turn, this decreases the effective cross section, which affects the elastic slope. Thus, the ratio of the damaged E to the undamaged E can qualitatively point out the degree of damage.

Figure 4 depicted typical stress-strain behavior curve for the tested pipes for both directions. As shown, pipe 5 exhibits the highest degree of preferred orientation as reflected by the microstructure. Pipe 3 displays almost no preferred directional property which is also supported by the uniform microstructure.

Figure 5a and b compare the plastic flow region for the tested pipes in both orientations. In the T orientation, the changes in the plastic flow behavior are more noticeable as compared to the L orientation. As mentioned, the banded ferrite-pearlite and the inclusions content are the more significant factors in influencing the strain hardening potential.

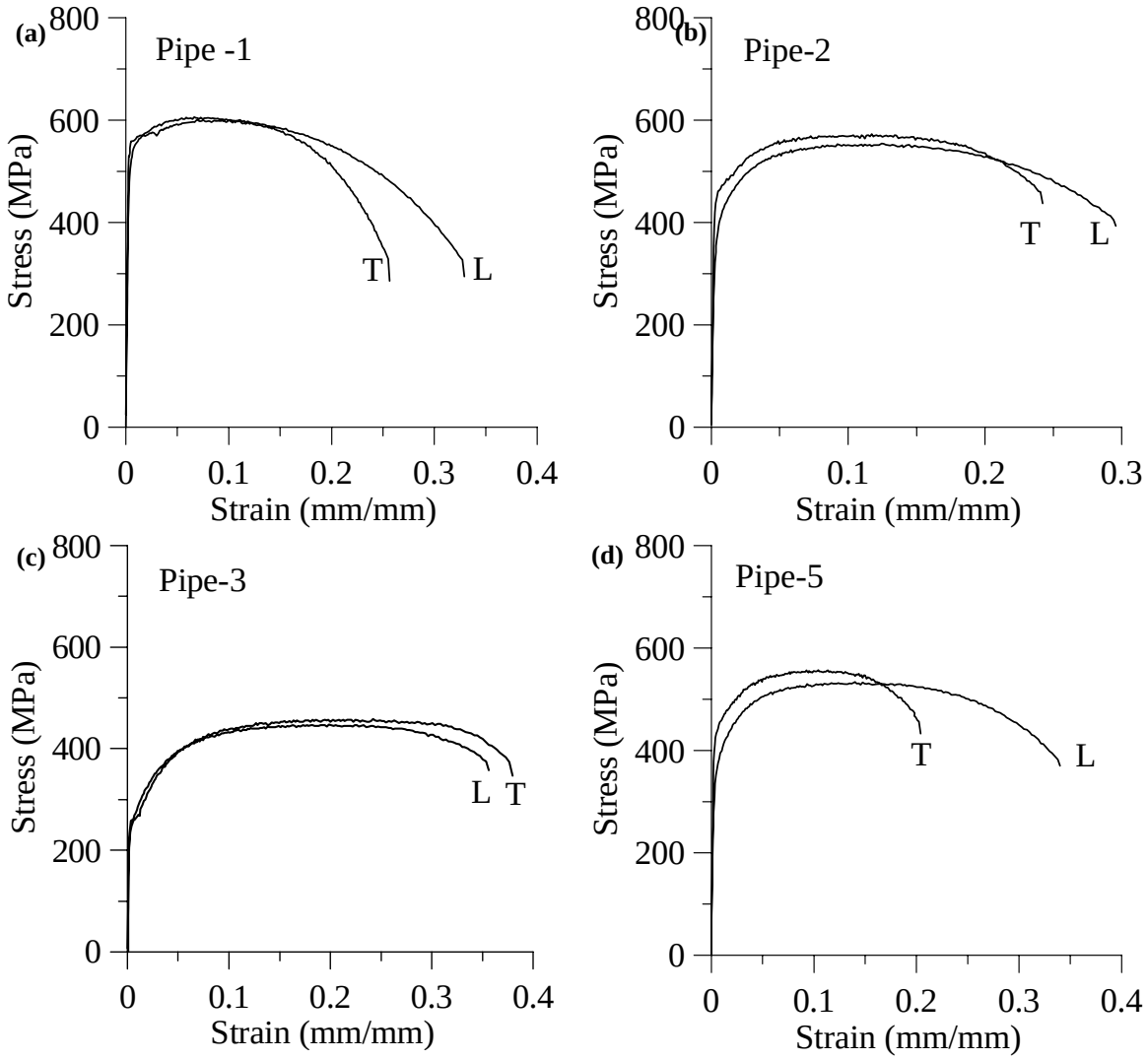

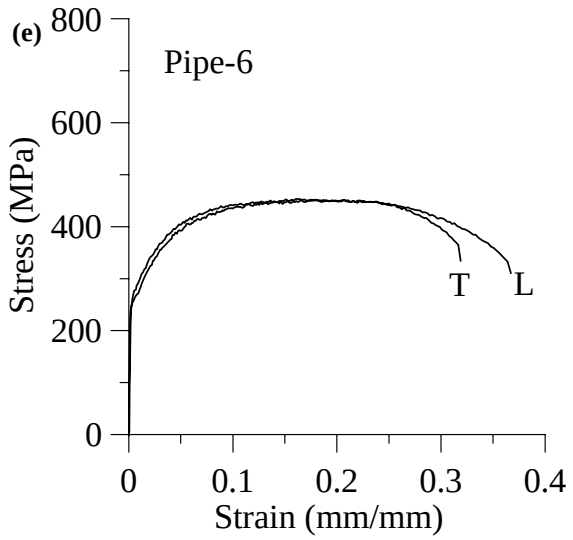

Figure 4. Stress-strain curves for the tested pipes in longitudinal and transverse orientations.

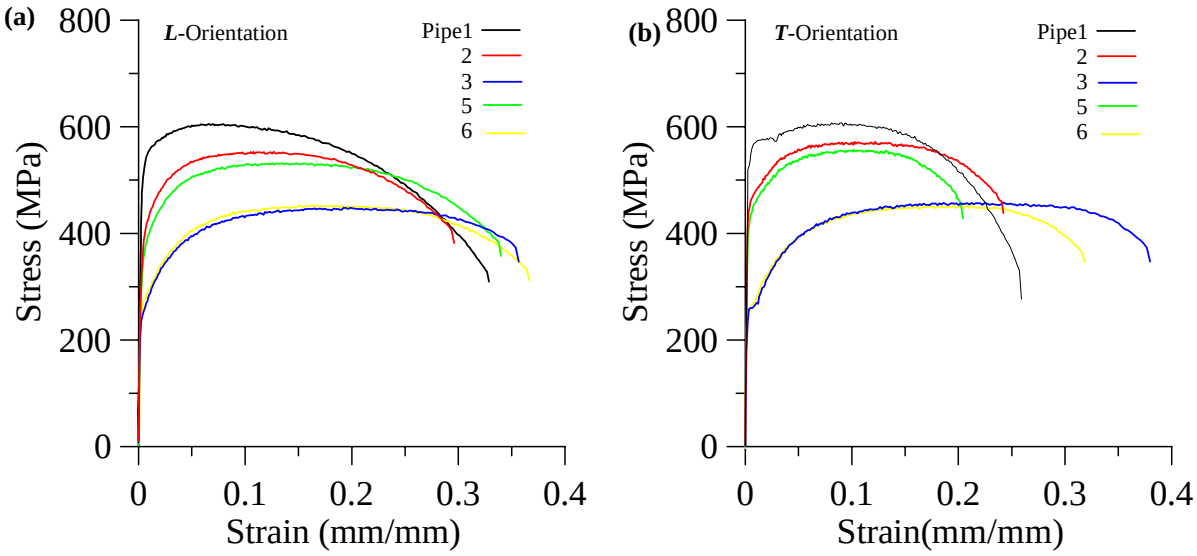

Figure 5. Comparison of the plastic flow for the various pipes as a function of orientation (a) L, (b) T.

Typical fatigue crack propagation results are shown in figure 6a and b for pipeline 2. This data compares well with published data from literature (Vosikovsky). Figure 7 and 8 show the macro fatigue fracture surfaces of the curved pipeline sections. The fatigue specimens were removed from the pipe and all fatigue cracks were initiated from electrical discharged machined center notches and propagated transverse to the pipeline longitudinal axis.

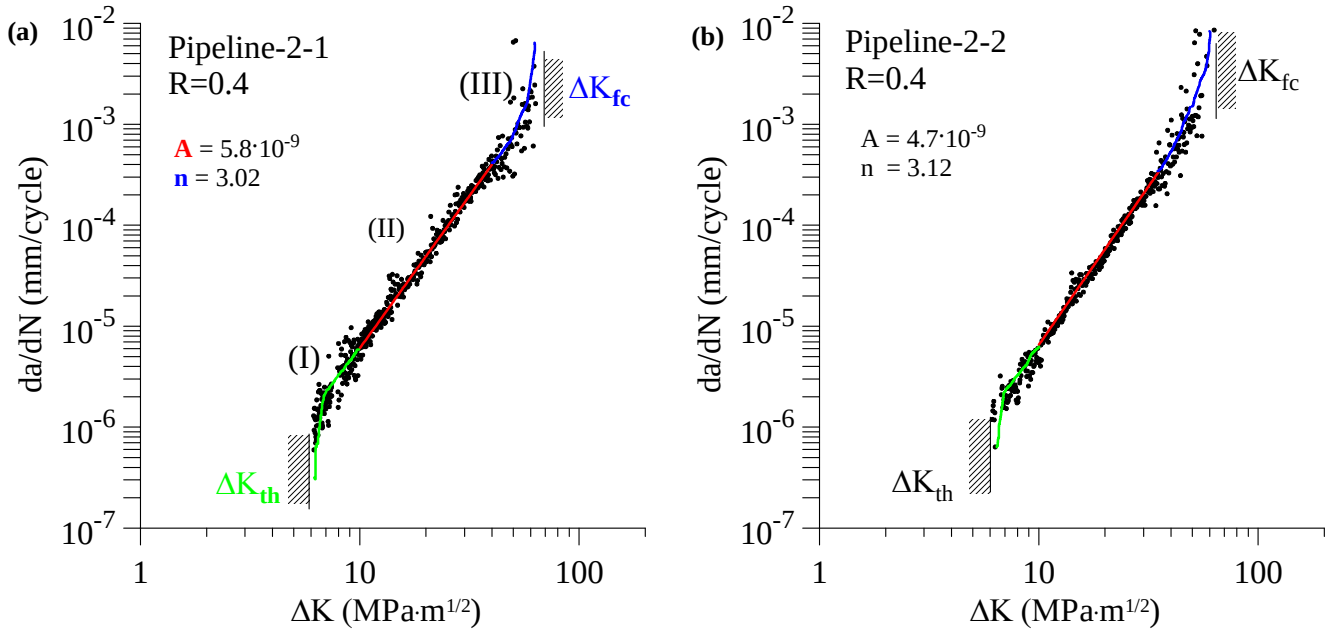

Figure 6 Fatigue crack propagation rate curves for pipeline 2 (a) spec. 1, (b) spec. 2.

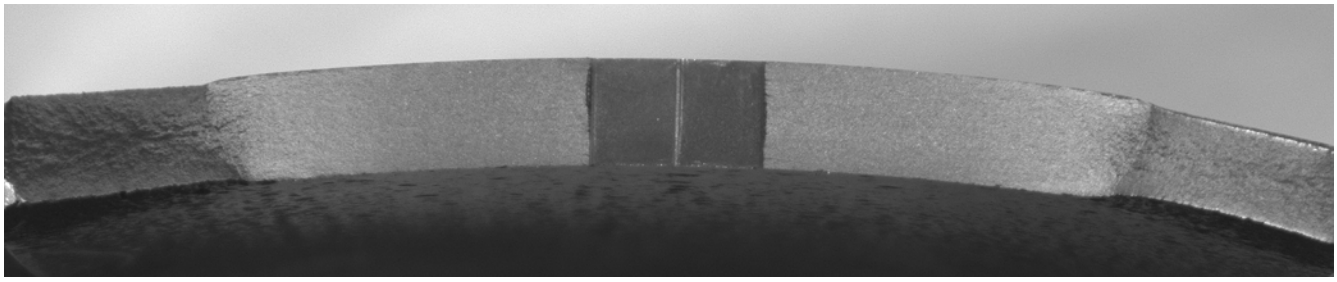

Figure 7. Macro fatigue fracture with emphasis on the symetrical crack front with some deviation at the later stage of fatigue crack growth.

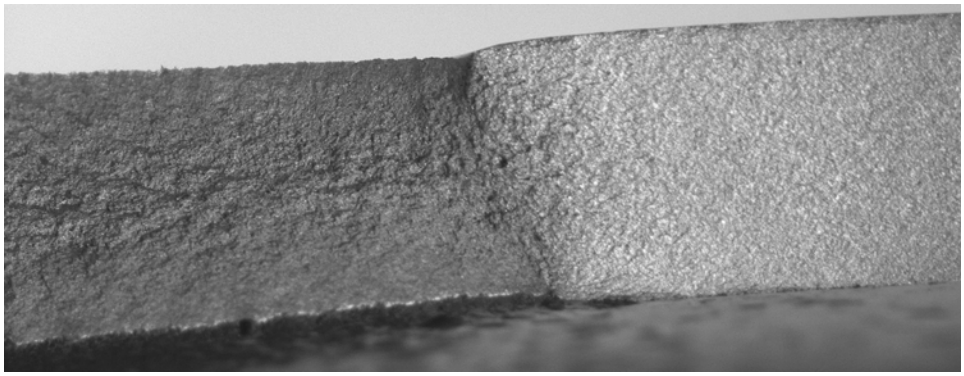

Figure 8. Macro fatigue fracture at the later stage accompanied by shear fracture mode resulting from monotonic loading.

CTOA results

Common Pipeline Steels

Figure 9 shows the crack tip location and the measurement made for the calculation of CTOA on some common, used and new pipeline steels. Figures 10a and 10b illustrate the CTOA curve profile with the crack extension. As shown there is a steep change of the CTOA value at the initial crack growth followed by a moderate change up to 5mm. From this point a stable CTOA was observed which actually characterized the critical CTOA, a material property similar to the fracture toughness parameter. Note the larger value of CTOA obtained while using all the images pictures (figure 10a) as compare to the one obtained while using every tenth image (figure10b). Figure 11 depicts the load-COD curve obtained during the CTOA test, accompanied by selected crack tip contour at different load level. As can be observed, progressive crack tip blunting occurs up to nearly the maximum load. Then crack initiation takes place followed by crack growth with almost no change in the load. This crack extension region is dominated by the normal stress field, which is reflected by ductile flat fracture mode (see figure 12a). This crack growth stage is followed by mixed mode crack growth, normally with shear (the dashed area limited by shear zones –figure 12b). This type of crack growth was accompanied by a slight decrease in load , then a full shear crack growth occurred (see figure 12b) (related to the stable CTOA) with a moderate decrease in load.

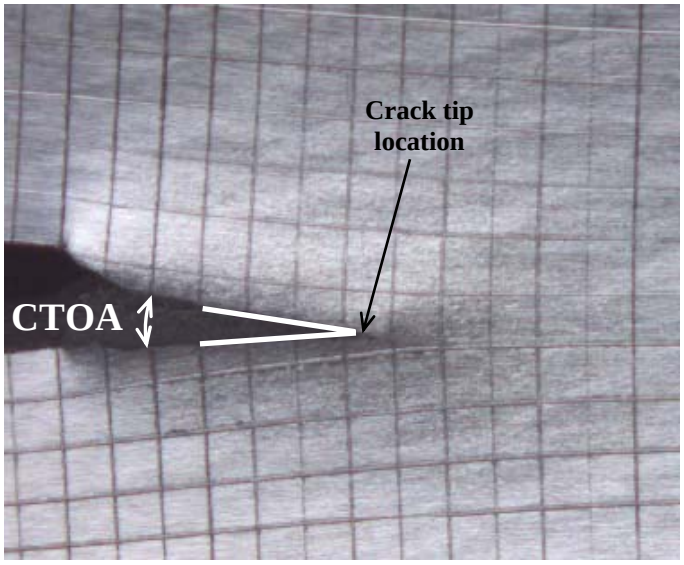

Figure 9. Crack tip location and CTOA measurement

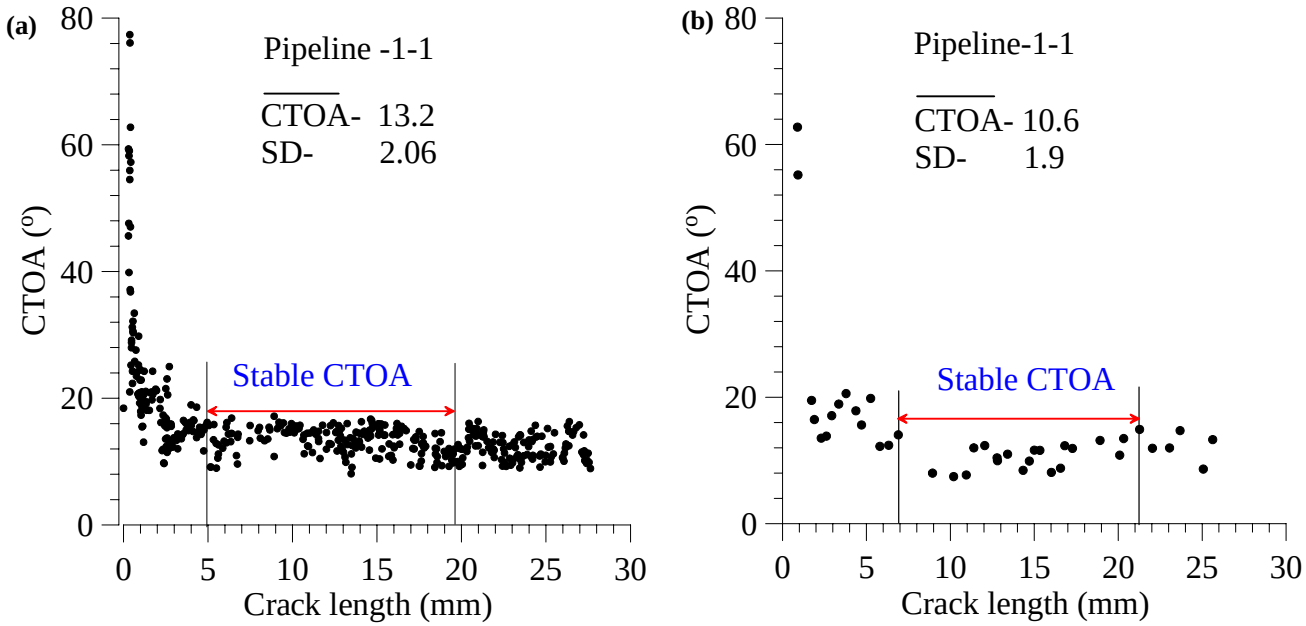

Figure 10. Mean CTOA value determined by using; (a) all the pictures, (b) every 10th picture.

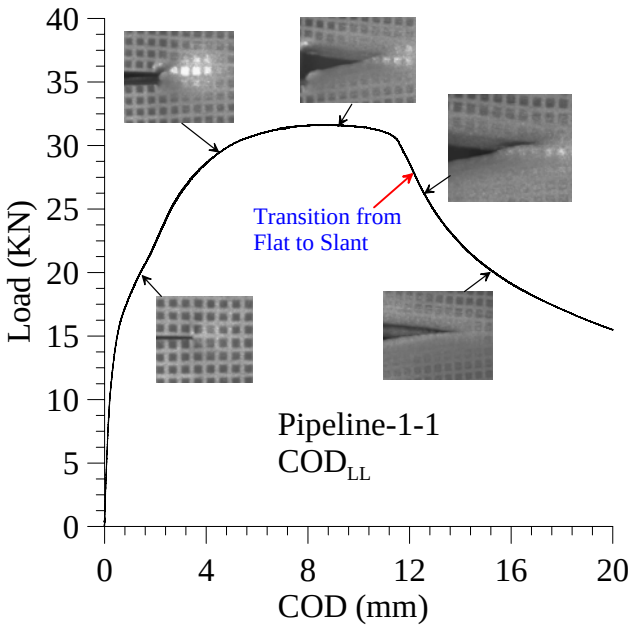

Figure 11. Load vs COD_{LL} curve and the change of crack tip profile during crack growth with loading. LL indicates that the COD gage was mounted at the load line

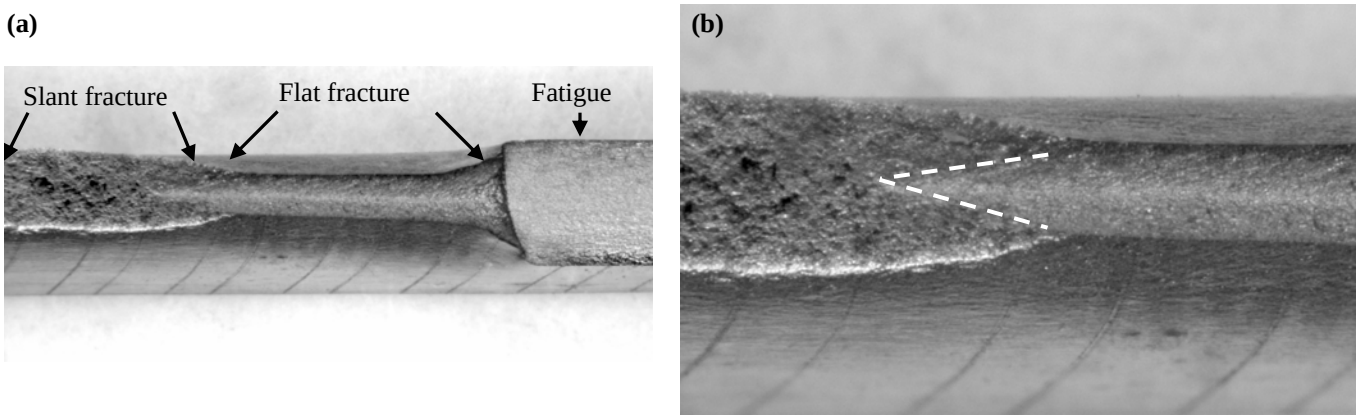

Figure 12. Macro fracture surface of a CTOA specimen indicating the transition from flat to slant fracture , (a) the various modes fracture, fatigue flat and slant, (b) and the transition fracture area.

X100 Pipeline Steel

Figure 13 illustrates the CTOA resistance curves for high strength pipeline steel (X100 steel). This figure represents the CTOA results from more than 125 images captured from two CTOA specimens.

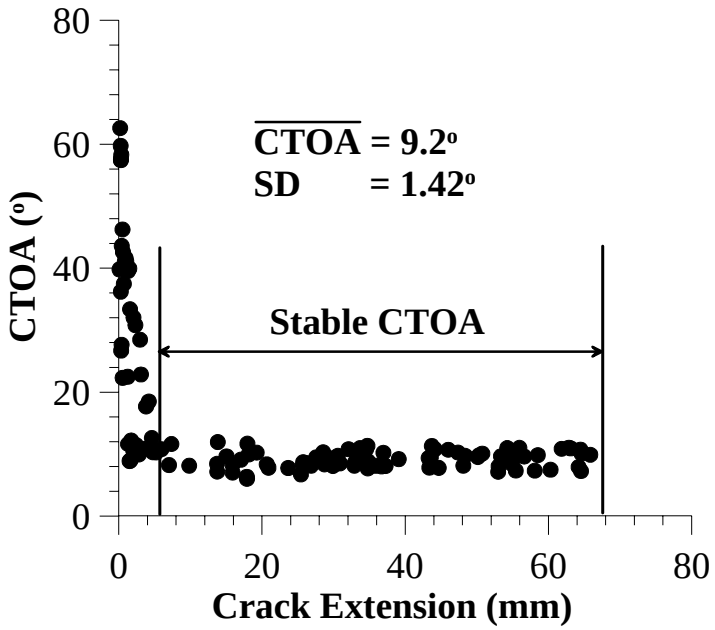

Figure 13. CTOA resistance curves for X100 steel

In Fig. 13, the initiation CTOA was high (around 60°) and it rapidly dropped in the flat-to-slant fracture transition region and approached a constant value (associated with steady state crack growth) at a crack length of 1.5 times the specimen thickness. Flat tearing and tunneling effects dominated the non-constant

CTOA profile during the early stages of crack growth. After the transition, full slant tearing (shear mode) was developed and resulted in a steady state CTOA value. The average maximum load reached in the two tests (steel # 5 corresponding to X100) was 59.6 kN, and the maximum crack velocity during the test reached 0.65 mm/s.

The CTOA resistance value of 9.2^o for the X100 steel is consistent with the CTOA data of 8.6^o reported by Hashemi et al. (measured with a similar quasi-static test technique, with specimen thickness of 8, 10 and 12 mm, and a similar measurement technique: an optical microscopy method with a digital video camera), for a different X100 steel. Furthermore, the comparison of the X100 results from the technique described here with those from drop-weight tear tests (Mannucci), that involve rapid loading values, and from tests on full pipes (Berardo) shows that the data are very comparable for each material class. Mannucci reported a CTOA value of 7^o (measured by two specimen tests) and 9.8^o (estimated by FEA), for a different X100 steel. Berardo reported CTOA results between 8.6^o and 9.6^o, measured from the displacement field behind the crack tip (reconstructed from the strain gauge records obtained during the full scale burst test for a different X100 steel). These data are encouraging and provide a better understanding of how the data from different test methods actually relate to each other.

FINITE ELEMENT ANALYSES

The critical CTOA fracture criterion and a two-dimensional elastic-plastic finite element analysis were used to calculate the maximum applied load and the crack extension behavior (the load-line displacement was also available but not presented here). The stabilized surface CTOA values, measured by optical microscopy, were used as the critical angle. Five different steels were evaluated for this analysis; three steels that were from used pipeline materials (#2 ,#3, and #4), one new steel from a mid-strength pipeline steel (#1) and one used (but never in service) X100 (#5) pipeline steel.

The load-line behavior for the CTOA-MDCB specimens are shown in Figs. 14 and 15.

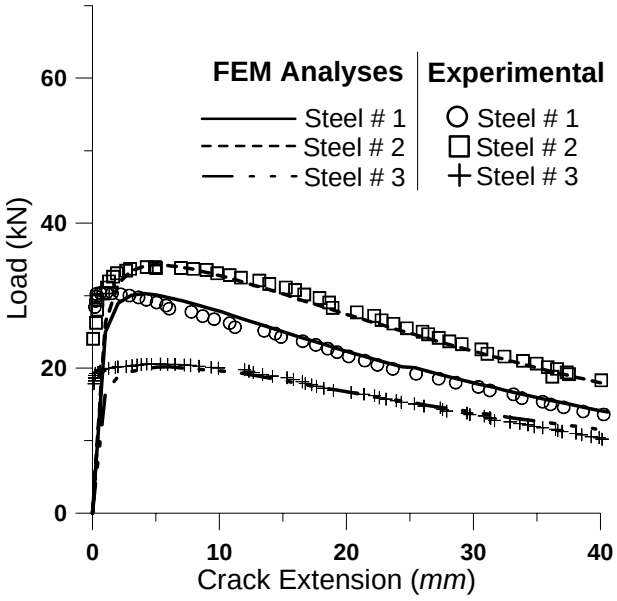

Figure 14. Load versus crack extension from experimental and FEM analyses for steels # 1-3 MDCB specimens

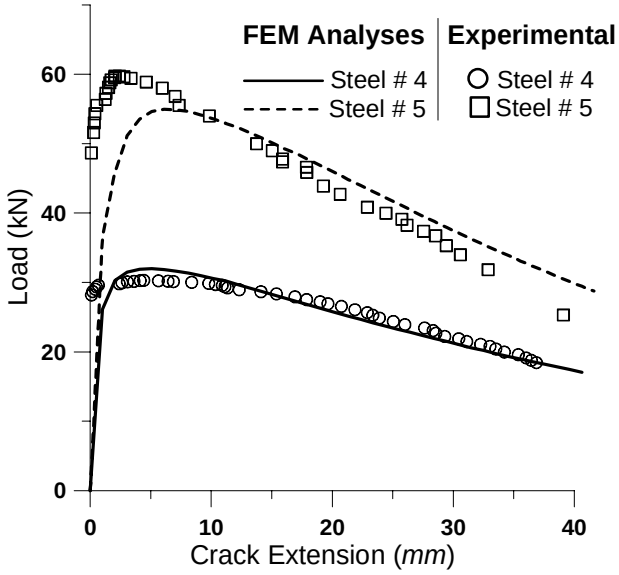

Figure 15. Load versus crack extension from experimental and FEM analyses for steels # 4-5 MDCB specimens

Table 3. Comparison between FEM calculated and measured results.

Steel #	Maximum loading (kN)			Correlation coefficient for curves
	Experimental data	FEM data	Relative error	
1	30.4	30.3	0.29 %	0.982
2	33.9	34.3	1.04 %	0.993
3	20.6	20.2	1.82 %	0.988
4	30.3	32.0	5.56 %	0.985
5	59.8	55.0	8.03 %	0.952

From the results shown in Figs.14 and 15 and in Table 3, several remarks can be made:

- The FEM calculated crack extension behavior (Figs. 14 and 15) for plane stress analysis (in the cracked region) agreed well with the experimental measurements. Correlation coefficients between the experimentally measured crack extension and the finite element analysis calculation for the 5 different steels tested lay between 0.952 and 0.993.
- The plane stress finite element calculation slightly underpredicted and overpredicted the experimentally measured maximum applied load at short and long crack extensions, respectively. The relative maximum load error was negligible for steels # 1-3, and increased with steel # 4 and 5. The relative error concerning the X100 steel (# 5) could be due to a misunderstanding of the steel mechanical properties (a stress-strain curve in the transverse direction may not be sufficient to take into account the specimen strain triaxiality behavior), or it could be due to stress triaxiality not taken into account in the 2D FEM simulations. This could be improved using new strain-stress characterization and 3D FEM simulations.
- The analyses tend to underpredict the initial crack extension when the crack extension is less than 6 mm (corresponding to twice the specimen thickness). This could be due to several factors:
  - the experimental measurements were made from surface observations and significant crack tunneling was shown to occur in this region;
  - during the phase between initiation and the attainment of maximum load, CTOA did not appear to be constant for these materials (some materials could have constant CTOA and others not during the flat-to-slant transition);
  - stress triaxiality could be a significant issue at the tip of the crack during the initial crack extension.

The two previous observations were not taken into account in the 2D simulation.

- The analyses accurately describe the crack extension behavior beyond the peak stress.
- Stress triaxiality is a significant issue at the tip of a crack even for thin sheet material. This stress triaxiality, or constraint, has received much attention in the past fifteen years by other researchers. The plane stress approximation has no constraint and the plane strain approximation introduces too much constraint (allowing the plane strain triaxiality to extend exceedingly far away from the crack tip). J.C. Newman modeled constraint, using the Plane Strain Core (PSC) concept, as a simple mixed state of stress with plane strain elements near the tip and plane stress elements away from the tip. The PSC concept in the 2D FEM CTOA simulations was not useful in our model. Indeed, the two thick loading arms (89.5 % of the finite element model), modeled with plane strain elements, appeared to balance the usual overestimation due to use of the plane stress elements. This is an interesting phenomenon and needs further investigation.